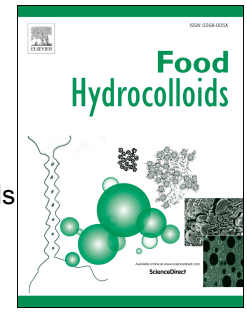

Effect of concentrations of alginate, soy protein isolate and sunflower oil on water loss, shrinkage, elastic and structural properties of alginate-based emulsion gel beads during gelation

Duanquan Lin, Alan L. Kelly, Valentyn Maidannyk, Song Miao

PII: S0268-005X(20)30100-4

DOI: https://doi.org/10.1016/j.foodhyd.2020.105998

Reference: FOOHYD 105998

To appear in: *Food Hydrocolloids*

Received Date: 15 January 2020

Revised Date: 25 April 2020

Accepted Date: 4 May 2020

Please cite this article as: Lin, D., Kelly, A.L., Maidannyk, V., Miao, S., Effect of concentrations of alginate, soy protein isolate and sunflower oil on water loss, shrinkage, elastic and structural properties of alginate-based emulsion gel beads during gelation, *Food Hydrocolloids* (2020), doi: https://doi.org/10.1016/j.foodhyd.2020.105998.

Graphical Abstracts

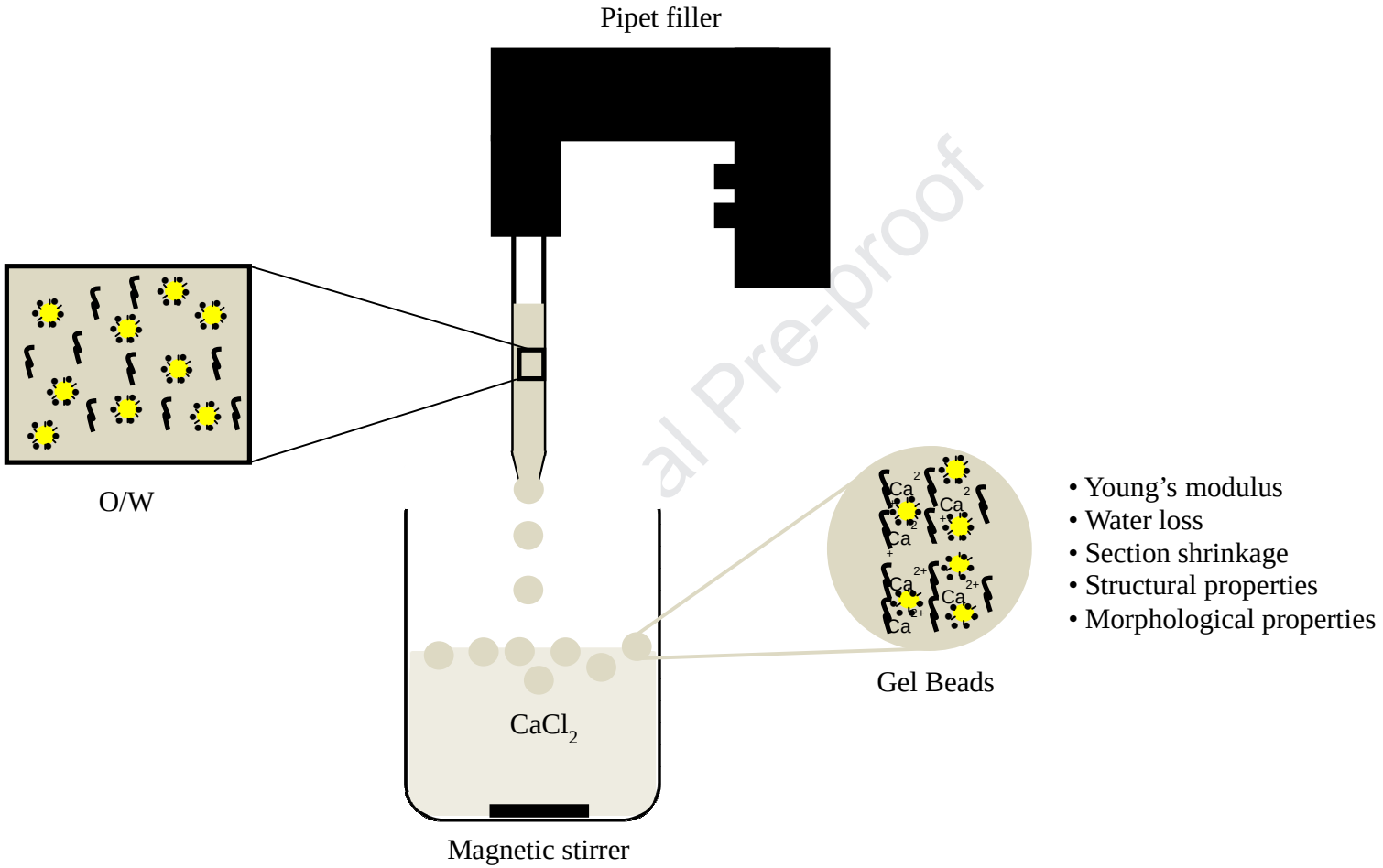

Effect of concentrations of alginate, soy protein isolate and sunflower oil on water loss, shrinkage, elastic and structural properties of alginate-based emulsion gel beads during gelation

Duanquan Lin[1, 2], Alan L. Kelly[2], Valentyn Maidannyk[1], Song Miao [1, 2, 3*]

[1]*Teagasc Food Research Centre, Moorepark, Fermoy, Co. Cork, Ireland*

[2]*School of Food and Nutritional Sciences, University College Cork, Cork, Ireland*

[3]*China-Ireland International Cooperation Centre for Food Material Science and Structure Design, Fuzhou, China*

*****Corresponding author

Dr. Song Miao

Tel: +353 2542468

Fax: +353 2542340

E-mail: song.miao@teagasc.ie

Abstract

The aim of this study was to investigate the influence of concentrations of sodium alginate (0.5%–1.5% in the water phase of an emulsion), soy protein isolate (SPI, 0.5%–2.0% in the water phase) and oil phase (10%–40% in the emulsion) on the properties (including water loss, shrinkage, morphological, elastic, and structural properties) of emulsion gel beads during gelation (0–30 min). Gel beads were prepared with external gelation by dropping emulsions into $CaCl_2$ solutions using pipettes. The Young's modulus of emulsion gel beads kept increasing during gelation before reaching a plateau accompanied by syneresis (i.e., water loss), shrinkage, and structural tightening. SPI absorbed at the surface of oil droplets could prevent re-coalescence of droplets during gelation. Additionally, increasing concentrations of sodium alginate and oil increased the Young's modulus of gel beads. Water loss decreased with increasing contents of alginate, SPI and oil, and shrinkage could be diminished by increasing alginate and oil contents.

Keywords: Alginate; Elastic property; Emulsion gel bead; Microstructure; Shrinkage; Soy protein isolates.

1. Introduction

Emulsion gels, also called emulgels, are a complex colloidal material which have some properties of both emulsions and gels (Dickinson, 2012). During the last decade, emulsion gels have received growing interest, due to their advantages compared to emulsions, such as higher storage stability by reducing oil and water phase movement and lipid oxidation (Ma, Wan, & Yang, 2017) and slower intestinal drug release, due to improved protective effects against gastric and intestinal phases (Corstens, Berton-Carabin, Elichiry-Ortiz, Hol, Troost, Masclee, et al., 2017; Guo, Bellissimo, & Rousseau, 2017). In order to produce emulsion gels, emulsions are first prepared by mixing gelling agent, emulsifier and oil and then turned into gels by different gelation mechanisms.

The choice of matrix material and emulsifier is the key factor in structuring emulsion gels. Proteins (e.g., soy protein isolate (SPI) and whey protein isolate (WPI)) and polysaccharides (e.g., agar and gellan gum) have been widely investigated as gelling agents in the formation of emulsion gels (Brito-Oliveira, Bispo, Moraes, Campanella, & Pinho, 2017; Geremias-Andrade, Souki, Moraes, & Pinho, 2017; Guo, et al., 2017). Different gelling agents can form different gelation structures, and the gelation mechanism (e.g., heat, high pressure, acidification, enzymatic treatment, and addition of ions) for different gelling agents differs (Dickinson, 2012), which can affect the properties of emulsion gels and encapsulated food nutrients. Both synthetic (e.g., Tween 80 and Span 80) and natural (e.g., proteins, egg lecithin, and soy lecithin) emulsifiers can be used to prepare emulsion gels. Lipid droplets in emulsion gels can be divided into active and inactive fillers according to the interactions between gelling agents and emulsifier-coated lipid droplets (Van Vliet, 1988; Yang et al., 2020), which can also influence the properties of emulsion gels (Geremias-Andrade, et al., 2017).

Alginate, a linear unbranched natural polysaccharide, is derived from brown seaweed extracts (*Phaeophyceae*) (King, 1983) and composed of two monomeric isomers: β-(1→4)-linked D-mannuronic acid (M) residues and α-(1→4)-linked L-guluronic acid (G) residues (Ching, Bansal, & Bhandari, 2017). Alginate-based emulsion gels received high attention in recent years (Lević, Pajić Lijaković, Đorđević, Rac, Rakić, Šolević Knudsen, et al., 2015; Qu, Zhao, Fang, Nishinari, Phillips, Wu, et al., 2016; Zeeb, Saberi, Weiss, & McClements, 2015). Alginate monomers can form gels by ionic crosslinking with divalent cations (mostly calcium cations in the food industry) (King, 1983). External gelation and internal gelation are two methods used to prepare alginate-based emulsion gels. Pintado, Ruiz-Capillas, Jimenez-Colmenero, Carmona, & Herrero (2015) added $CaSO_4$ into an alginate-based emulsion to directly produce an alginate-based emulsion gel. Sato, Moraes, & Cunha (2014) used internal method to produce emulsion gels, in which CaEDTA was added to an alginate-based emulsion first, after which acid was introduced to liberate calcium ions. Compared these two methods, Puguan, Yu, and Kim (2014) found that gels formed by external gelation had a smoother surface and denser inner structure. In addition, alginate-based gels are not sensitive to gastric fluids, and can protect the encapsulated nutrients from harsh gastric environment, and the remaining gel structures can be further disrupted during intestinal digestion accompanied by the release of encapsulated compounds (Zhang, et al., 2016).

Previous studies mainly focused on the formulation, structural properties, mechanical properties, stability, and digestion of alginate-based emulsion gels. However, there are few reports on the gelation process of alginate-based emulsion gels. It has been indicated that, during the gelation process of alginate hydrogels prepared by external gelation, calcium cations can diffuse into alginate drops after being dropped into a calcium chloride solution (Rehm, 2009). Syneresis also occurs during this gelation process, with a consequent decrease in dimensions of gel beads (Quong, Neufeld, Skjåk-Bræk, & Poncelet, 1998; Rehm, 2009).

However, the gelation process of alginate-based emulsion gels may differ from that of alginate gels, because the presence of lipids and emulsifers in emulsions may affect the gelation process. Understanding the gelation process of alginate-based emulsion gels may help to produce emulsion gels with specific properties (e.g., size, water content, mechanical properties) by controlling gelation time, formulation, preparation methods and processing technologies. Therefore, further studies are needed to understand how alginate, emulsifiers and oil affect the gelation process of emulsion gel beads.

The purpose of this study was thus to investigate the gelation process of alginate-based emulsion gel beads. In order to improve the encapsulation efficiency and hygroscopicity of alginate-based emulsion gels, proteins (e.g., lupin protein and WPI) can be used as emulsifiers (Corstens, et al., 2017; Piornos, Burgos-Díaz, Morales, Rubilar, & Acevedo, 2017), and polysaccharides (e.g., *Prosopis alba* exudate gum and chitosan) can be used as structural strengthening agents (Natrajan, Srinivasan, Sundar, & Ravindran, 2015; Vasile, Judis, & Mazzobre, 2018). In this study, denatured SPI was thus introduced as surfactant, because SPI has a huge potential value in producing emulsion gels, due to its good emulsifying property, and denatured SPI has increased emulsifying capacity compared to natural SPI (Lin, Lu, Kelly, Zhang, Zheng, & Miao, 2017; Nishinari, Fang, Guo, & Phillips, 2014). In addition, the external gelation was used, in order to obtain gel beads with denser structures, compared to internal gelation. Effect of concentrations of alginate, SPI, and sunflower oil on the shrinkage, water loss, elastic and structural properties of alginate-based emulsion gel beads during gelation were investigated in this study.

2. Materials and methods

2.1. Materials

Defatted soy flour (Bob's Red Mill, Milwaukie, Oregon, USA) and sunflower oil (Aldi Stores Ltd., Kildare, Ireland) were purchased from iHerb and Aldi, respectively. Sodium alginate was obtained from Special Ingredients (Chesterfield, UK). Calcium chloride, sodium hydroxide, and hydrochloric acid were purchased from Sigma-Aldrich (St. Louis, MO, USA).

2.2. Preparation of soy protein isolate

SPI was prepared according to the method described by Urbonaite, Jongh, Linden and Pouvreau (2015). The defatted soy flour was suspended in distilled water at a ratio of 1:10 (w/w) at 45 ºC and stirred for 30 min. The pH value was then adjusted to 8.0 with 5 M NaOH, and the solution was stirred for 30 min in the water bath. The supernatant was collected by centrifugation (30 min, 6000×g, 13 ºC) (Sorvall LYNX 6000 Superspeed Centrifuge, Thermo Fisher Scientific, Waltham, USA). Protein isolates were obtained by isoelectric precipitation by adjusting the pH value to 4.5 with 6 M HCl. After mild stirring for 12 h at 5 ºC, the suspension was centrifuged (30 min, 6000×g, 7 ºC). The sediment was re-suspended three times in deionized water at a ratio of 1:3 (w/w) and filtered by multilayer gauze to remove any remaining insoluble material, and the filtrate was centrifuged (30 min, 6000×g, 7 ºC) again. The sediment was finally suspended in deionized water at a ratio of 1:4 (w/w), and the pH value was justified to 7.0 with 5 M NaOH. Then, the solution was freeze-dried (Free Zone 12 Freeze Dry System, Labconco Corpotation, Kansas, MO, USA). The dried SPI was kept in polyethylene bags and stored at room temperature. The protein content of SPI powder was 96.29 ± 0.03%.

2.3. Preparation of alginate-based and SPI-stabilized emulsions and gel beads

A dispersion of soy protein isolate (5% wt in distilled water) was stirred at room temperature for 30 min using a magnetic stirrer, heated at 90 ºC for 30 min, and then cooled to room temperature. For the production of continuous phase, sodium alginate (0.5, 1.0, and 1.5% wt)

was added into the pre-heated soy protein isolate solution with adding water to reach final concentrations of SPI (0.5, 1.0, and 2.0% wt) by shearing at 400 rpm for 30 min with a magnetic stirrer and then allowed to rest for 24 h to permit hydration. For the production of o/w emulsion, sunflower oil (10, 20, and 40% wt) was added to above continuous phase and mixed at 18,000 rpm for 2 min with an Ultra-Turrax (IKA-25, Staufen, Germany). Solutions containing 1.0% alginate (1A) and dispersions containing 1.0% alginate and 1.0% SPI (1A1S) were prepared as control groups without mixing at 18,000 rpm for 2 min. Table 1 shows the formulations used for preparing emulsions.

For producing gel beads, the resulting dispersions/solutions were dropped into 2 % (w/w) $CaCl_2 \cdot 2H_2O$ solutions using 5-ml measuring pipettes and a S1 pipette filler (Thermo Fisher Scientific Inc., Waltham, USA). The distance between the tip of pipette and the surface of $CaCl_2$ solutions was fixed at 10 cm. The samples were allowed to gel in $CaCl_2$ solutions for 30 min with mild magnetic stirring, and the resulting beads were rinsed with distilled water. Samples were analyzed immediately for measurement of Young's modulus, shrinkage, water loss, and morphology, and samples were kept in distilled water for observing their structures within 3 hours after being prepared.

2.4. Properties of dispersions/solutions

2.4.1. Structures

Confocal scanning laser microscopy (CLSM) was used to observe microstructures of dispersions/emulsions. Dispersion/emulsion samples (500 µl) were transferred to a glass slide and stained with 50 µl of a mixture of Nile red (0.1%, w/v, in polyethylene glycol-200) and fast green (0.1%, w/v, in distilled water) at a ratio of 3:1. Confocal observation was performed using a Leica TCS SP5 microscope (Leica Microsystems GmbH, Wetzlar,

Germany) at excitation and emission wavelengths of 488 nm and 633 nm, provided by an argon laser and a HeNe laser, respectively.

2.4.2. Viscosity

The viscosity of dispersions/solutions was tested at 25 ºC using an AR 2000ex rheometer (TA Instruments, Crawley, UK) with an aluminium parallel plate (60 mm in diameter, and 0.5 mm in gap). Each sample was added in the middle of Peltier plate and allowed to stand for 2 min before testing. The flow measurement was performed over a shear rate range of 0.1 to 100 s^{-1}, and viscosity (η) was obtained from the data analysis software.

2.5. Microstructures of gel beads

CLSM was used to observe microstructures of gel beads. Each gel bead was cut into a thin layer (~ 1 mm), transferred to a glass slide, and stained with a mixture of Nile red (0.1%, w/v, in polyethylene glycol-200) and fast green (0.1%, w/v, in distilled water) at a ratio of 3:1. Confocal observation was performed by the method described in section 2.4.1.

2.6. Young's modulus of gel beads

The Young's modulus of gel beads during gelation at 1, 2, 3, 4, 5, 6, 8, 10, 20, and 30 min were analysed by a TA.XT Plus texture analyser (Stable Micro System, Godalming, UK) according the method described by Ching, Bansal, & Bhandari (2016) with a minor change. The surface of samples was dried with dry paper before testing. Compression tests were performed using a cylinder probe of 10-mm diameter and a 5-kg load cell. The samples were compressed to 30% strain at a crosshead speed of 0.1 mm/s, and five beads with same composition were examined one after another. Due to their ellipsoidal shapes, the cross-sectional area of samples was calculated after measuring the major axis and minor axis of samples after being placed on the platform of texture analyser. The Young's modulus of each

sample was calculated as the gradient of the stress vs. strain curve in the 5–15% strain region, where stress and strain showed good linearity. The experiment was performed in triplicate.

2.7. Water loss of gel beads

The water loss of samples during gelation was determined at 1, 2, 3, 4, 5, 6, 8, 10, 20, and 30 min after dispersions/solutions were dropped into calcium chloride solutions. In this study, the water loss means the decreased water in gel beads during gelation compared to the original dispersions/solutions. Five gel particles were obtained from calcium chloride solutions and washed with distilled water. After drying the surface, the initial weight of 5 beads was weighted (W'_i) and then they were dried in an oven at 80 ºC until constant weight (W'_d). The initial weight (W_i) and the weight after drying (W_d) of dispersions/solutions (5 drops) were determined by the same method. Thus, the water loss was calculated from Eq. (1), if we assumed that the main content (i.e., alginate, SPI, and oil) of gel beads have no significant change during gelation, and the experiment was replicated three times.

$$\text{Water loss}\ (\%) = \left(\frac{W_i - W_d}{W_i} - \frac{W_d}{W_i} \times \frac{W'_i - W'_d}{W'_d}\right) \times 100\% \qquad (1)$$

2.8. Shrinkage of gel beads

The section shrinkage rate of gel beads was determined at 2, 4, 6, 8, 10, 20, and 30 min after dispersions/solutions were dropped into calcium chloride solutions. Five gel beads were obtained from the calcium chloride solutions and washed with distilled water. After drying the surface, photographs of gel beads were taken using a camera (iPhone 7 plus, Apple Inc., California, USA). The major semi-axis (r'_{max}) and minor semi-axis (r'_{min}) of gel beads were measured by using a digital vernier calliper, and the section area (A'_s) was calculated from Eq. (2). The major semi-axis (r_{max}) and minor semi-axis (r_{min}) of gel beads after gelation for 1 min were measured, and the section area (A_s) was also calculated from Eq. (2). The section

shrinkage rate of gel beads was calculated from Eq. (2), and the experiment was replicated three times. It should be noted that the section shrinkage rate of samples during gelation process was compared to the section area of samples after gelation for 1 min in this study.

$$Section\ shrinkage\ rate\ (\%) = \frac{A_s - A'_s}{A_s} = \frac{3.14 \times r_{max} \times r_{min} - 3.14 \times r'_{max} \times r'_{min}}{3.14 \times r_{max} \times r_{min}} \times 100\% \quad (2)$$

3. Results and discussion

3.1 Structural properties of gel beads

Structural properties are important for emulsion gels because they can influence mechanical properties of emulsion gels and release behavior of encapsulated nutrients. Many factors (e.g., structures of the gel matrix, structures of emulsion droplets, and interactions between the gel matrix and droplets) can influence the structures of overall emulsion gels. Therefore, the effect of concentrations of alginate, SPI and oil on the structures of emulsions and emulsion gels was investigated in this study.

Fig. 1 shows the structures of emulsions/dispersions before gelation and gel beads after gelation for 30 min. In sample 1A1S, SPI formed aggregates and dispersed in alginate solutions (Figs. 1A and 1V). This was because SPI was heated at 90ºC for 30 min in this study, and thus the solubility of SPI decreased, due to denaturation; additionally, denatured SPI exposed hydrophobic residues and thus formed aggregations in alginate solutions (Wagner & Añón, 1990). After mixing the 1A1S dispersion with oil, SPI modules can move from the continuous phase to the O/W interfaces and are absorbed at the surface of oil droplets (Figs. 1A and 1B), due to their amphipathic nature and emulsifying capacity. Hydrophobic groups of SPI absorbed onto the surface of oil droplets, and hydrophilic groups connected with the water phase, acting as a steric barrier against coalescence of oil droplets (Nishinari, et al., 2014). However, increasing the alginate concentration to 1.5% led to more

SPI aggregations in the water phase (Figs. 1B and 1C), because the higher viscosity of the continuous phase of emulsions hindered SPI from moving to the oil–water interface (Tavernier, Patel, Van der Meeren, & Dewettinck, 2017). Higher SPI concentrations resulted in more SPI being absorbed at the surface of oil droplets but led to more obvious flocculation of oil droplets (Figs. 1B and 1D), probably due to the depletion flocculation of droplets coated by excessive amount of SPI (Moschakis, Murray, & Biliaderis, 2010). In addition, increasing oil content of emulsions resulted in more compacted gel structures (Figs. 1B and 1E), due to the decreased ratio of the water phase to the oil phase.

Fig. 1 also indicates that there were more dark sections in emulsions/dispersions than gel beads in all samples, which indicates that syneresis and shrinkage of the water phase during gelation led to more compact filler structures. In addition, the concentrations of SPI, alginate and oil could affect the stability of droplets during gelation. As shown in Figs. 1B and 1W SPI-coated droplets in sample 1A1S20O could maintain their structures during gelation. This was because SPI could stabilize the o/w emulsions, and gelation, syneresis and shrinkage mainly occurred in the water phase during gelation, which had no significant effects on the structures of emulsion droplets. Similarly, it was found that WPI-aggregate-stabilized emulsions were stable during the gelation period (Rosa, Sala, Van Vliet, & Van De Velde, 2006). Additionally, higher SPI concentration resulted in more stable droplet structures during gelation, probably because of more SPI being absorbed at the surface of oil droplets (Figs. 1D and 1Y). However, increasing the alginate concentration to 1.5% led to re-coalescence of droplets during gelation (Figs. 1C and 1X), because increased viscosity of the continuous phase of emulsions hindered SPI from moving to the oil–water interface and thus resulted in decreased stability of emulsion droplets during gelation. In addition, increasing the oil content to 40% also led to re-coalescence of droplets during gelation (Figs. 1E and 1Z), probably because 1.0% SPI in the water phase was not enough to stabilize 40% oil.

3.2. Young's modulus of gel beads

3.2.1. The profiles of Young's modulus during gelation

Compression tests were carried out to study the elastic properties of gel beads during gelation. Firstly, the effect of introducing SPI and oil into alginate gels on the profiles of Young's modulus during gelation was investigated. As shown in Fig. 2A, the changes of Young's modulus of gel beads containing 1% alginate (1A in short) included three steps: increasing up to 5 min, decreasing between 5 and 10 min, and then reaching a plateau. The Young's modulus of gel beads containing 1% alginate and 1% SPI (sample 1A1S) had a similar trend to that of sample 1A, but the Young's modulus of emulsion gel beads containing 1% alginate, 1% SPI, and 20% oil (sample 1A1S20O) increased first and then reached a plateau at 8 min directly (Fig. 2A). It can be seen that the gelation process of alginate-based gel beads includes the maturation step (increased Young's modulus), the structural collapse step (decreased Young's modulus), and the equilibrium step (unchanged Young's modulus). Therefore, it was assumed that the gelation mechanism of alginate beads prepared by the external gelation has a direct effect on the changes in Young's modulus during gelation.

After being dropped into calcium chloride solutions, the surface of alginate drops can gel instantaneously, and then Ca^{2+} can diffuse from the $CaCl_2$ solutions into the interior of alginate drops, which leads to the gelation of gel beads from outside to inside and increased Young's modulus (Ching, et al., 2017). This process is called the maturation step (Puguan, et al., 2014). The concentration of alginate solutions and the size of gel beads are the main factors affecting the Ca^{2+} diffusion into alginate gel beads during gelation. It has been reported that higher alginate concentrations incorporated more calcium ions in alginate gel beads (Quong, et al., 1998). In this study, all gel beads were prepared with 2% (w/w) $CaCl_2 \cdot 2H_2O$ solutions, and the size of samples 1A (r_{max} = 2.1 mm and r_{min} = 2.0 mm), 1A1S

(r_{max} = 2.2 and r_{min} = 2.1), and 1A1S20O (r_{max} = 2.1 and r_{min} = 2.0) did not significantly differ at the end the maturation step. Therefore, it was assumed that the changes in Young's modulus of samples 1A, 1A1S, and 1A1S20O during the maturation step showed a similar trend probably because oil and SPI had no significant effect on the Ca^{2+} diffusion from the $CaCl_2$ solutions in alginate gel beads during the maturation step.

After the maturation step, the Young's modulus of samples 1A and 1A1S decreased before reaching a constant value (Fig. 2A). The concentrations of Ca^{2+} and alginate in alginate gel breads decreases from the gel surface to gel core (Quong, et al., 1998), which indicates that the gel structure of the outer regions of beads is stronger than that of inside gel beads. Therefore, the fragile core structure of gel beads can not support the whole structure, which leads to the collapse of the inner structure at the end of the maturation step and thus a decreased Young's modulus (Puguan, et al., 2014). However, the Young's modulus of sample 1A1S20O reached the balance directly after the maturation step during gelation (Fig. 2A). This was probably because the structures of sample 1A1S20O are totally different from that of samples 1A and 1A1S. After introducing oil into 1A1S dispersions, oil droplets disperse in the alginate solutions during homogenization, and SPI molecules move to the surface of oil droplets from the water phase, due to their emulsifying capacity. The resulting emulsions can turn into emulsion gels after alginate monomers are crosslinked by calcium cations, and shrinkage also occurs during this process. However, oil droplets may act as fillers and help to support the structure of gel beads from collapse after the maturation step during gelation. It has also been indicated that the oil core could support the shell of silica gels from fracture during the sol-gel process (Liang, Liu, Zhang, Qu, Li, & Yang, 2011). Therefore, it was also assumed that oil played an important role on preventing the structural collapse of alginate gel beads during gelation.

The effect of concentrations of alginate (Fig. 2B), SPI (Fig. 2C) and sunflower oil (Fig. 2D) on the profiles of Young's modulus of emulsion gel beads during gelation was further investigated. Fig. 2B shows that the Young's modulus of sample 0.5A1S20O increased initially, decreased between 4 and 8 min, and then increased again, before reaching a plateau. In this sample, the structure of gel matrix formed by 0.5% alginate is fragile during the maturation step, which results in severe structural collapse before compact emulsion droplets can support emulsion gel structures. However, samples 1A1S20O and 1.5A1S20O showed a similar trend, in which the Young's modulus increased up to 8 min and then reached a plateau (Fig. 2B). This indicates that increasing alginate concentrations from 0.5% to 1.5% not only slowed Ca^{2+} diffusion and thus caused a slowing of the maturation step but also formed stronger alginate-based matrix structures and thus protected emulsion gel structures from collapse during gelation. Figs. 2C and 2D show that increasing SPI concentrations from 0.5% to 2.0% and oil contents from 10% to 40% had no significant effect on the profiles of Young's modulus during gelation (i.e., reaching the plateau directly after the maturation step at around 8 min during gelation). This was probably because increasing concentrations of SPI and oil had no significant impact on calcium diffusion in emulsion gel beads, and 10% oil was high enough to prevent structural collapse of emulsion gel beads after the maturation step during gelation.

3.2.2. Effect of alginate, SPI and oil on the Young's modulus of gel beads after gelation

Mechanical properties are important for emulsion gels because they are closely associated with other properties (e.g., storage stability, oral perception, and controlled release of encapsulated nutrients). Many factors can affect mechanical properties of emulsion gels, such as gel strength of gel matrix structures (i.e., protein and polysaccharide), modulus of filler droplets, and interactions between oil droplets and the gel matrix. Therefore, the effect of concentrations of alginate, oil and SPI on the Young's modulus of emulsion gel beads was

316 investigated in this study, and all samples were compared after they were allowed to gel for
317 30 min in $CaCl_2$ solutions (Figs. 2B–D).

318 Fig. 2B shows that increasing alginate concentrations from 0.5 to 1.5% significantly
319 increased the Young's modulus of emulsion gel beads. This was expected because increasing
320 alginate concentration could increase gel strength of alginate-based gel matrix and thus
321 increase the Young's modulus of overall emulsion gels. Similarly, it has previously been
322 reported that increasing agar content (from 1.0 to 1.8%) in o/w emulsions containing 0.1
323 volume fraction of corn oil decreased the overall volume of void spaces and increased strand
324 compactness of emulsion gels (Kim, Gohtani, Matsuno, & Yamano, 1999).

325 Fig. 2D indicates that increasing oil contents from 10% to 40% had no significant effect on
326 the Young's modulus of emulsion gel beads. According to the interactions between
327 emulsifier-coated emulsion droplets and the gel matrix, oil droplets can be divided into active
328 and inactive fillers (also known as bound and unbound fillers) in emulsion gels (Dickinson,
329 2012; Yang et al., 2020). Active fillers are mechanically connected to the gel network by
330 noncovalent and/or covalent bonds through emulsifiers. For examples, it has been reported
331 that WPI-coated oil droplets could be bound to a WPI-based gel matrix by covalent
332 interactions (e.g., hydrophobic interactions and sulphur bridges) (Sala, de Wijk, van de
333 Velde, and van Aken, 2008); it has been also indicated that lactoferrin-stabilised emulsion
334 droplets could bind to a κ-carrageenan gel, probably because of electrostatic interactions
335 between positively charged lactoferrin (pI = 8.2) and negatively charged κ-carrageenan at pH
336 7–8 (Sala, van Vliet, Cohen Stuart, Aken, and van de Velde, 2009). In addition, the Kerner
337 model can explain the effect of active fillers on the mechanical properties of emulsion gels
338 (Kerner, 1956). According to this model, increasing the volume fraction (ϕ_f) of active fillers
339 can increase the mechanical properties of emulsion gels, which has been supported by many
340 studies (Oliver, Berndsen, van Aken, & S□holten, 2015; Sala, et al., 2009). However, in this

study, SPI (pI = 4.5) and alginate were both negatively charged at pH 6.5–7.0, so there are no electrostatic interactions between SPI-coated droplets and alginate-based gel matrix. It is also unlikely that SPI-coated droplets can connect to the alginate-based gel network by covalent interactions. Additionally, the results obtained in this study were in a disaccord with the Kerner model. Therefore, it was assumed that SPI-coated droplets were inactive fillers in alginate-based emulsion gel beads.

Fig. 2C shows that increasing SPI concentrations decreased the Young's modulus of emulsion gel beads. According to the state of emulsion droplets in gels, structures of emulsion gels can be divided into two categories: emulsion droplet-filled gels and emulsion droplet-aggregated gels (Dickinson, 2012). In emulsion droplet-filled gels, the continuous phase (e.g., protein- and polysaccharide-based gels) forms a continuous gel matrix, and emulsion droplets are embedded in this gel matrix. In emulsion droplet-aggregated gels, emulsion droplets aggregate together and form a network structure, such that the gel matrix is disrupted by the aggregated emulsion droplets. As shown in Figs. 1B and 1D, more aggregations of emulsion droplets occurred in sample 1A2S20O compared to sample 1A1S20O, probably because increasing SPI concentration led to more depletion flocculation of SPI-coated droplets in emulsions (Lam & Nickerson, 2013). In active droplet-aggregated gels, the crowding effect of fillers (particle interactions) increases the shear modulus of the overall gels (Oliver, et al., 2015). However, SPI-coated droplets in alginate-based gel matrix may act as inactive fillers as disccussed before in this study. Therefore, it was assumed that increased aggregation of SPI-coated droplets (inactive fillers) had a negative effect on the Young's modulus of alginate-based emulsion gel beads, probably because aggregated droplets (i.e., the increased phase separation between alginate-based gel matrix and SPI-coated droplets) may disturb the formation of alginate-based network structures (Dickinson, 2012; Lin, Lu, Kelly, Zhang, Zheng, & Miao, 2017).

366 *3.3 Water loss of gel beads*

367 During the maturation step, inter-chain interactions between stretches of alginate monomers
368 and Ca^{2+} occurred with the diffusion of Ca^{2+} from the surface to interior of gel beads, and the
369 formation of junctions between these stretches forced water out, which led to shrinkage and
370 increased water loss of gel beads during gelation (Puguan, et al., 2014; Rehm, 2009). Fig. 3
371 shows the effects of concentrations of alginate, SPI, and oil on the water loss from emulsion
372 gel beads during gelation. It indicates that increasing alginate contents (from 0.5 to 1.5%) or
373 SPI concentration (from 0.5 to 2.0%) had no significant effect on the rares of water loss, but
374 increasing oil content (from 10 to 40%) could slow the water loss in terms of the profiles of
375 water loss during gelation, probably because lower water content of the original emulsions
376 results in slower water loss of emulsion gels during gelation.

377 Fig. 3 also indicates that the water loss of emulsion gel beads after gelation for 30 min
378 decreased with increasing alginate contents (from 0.5 to 1.5%), SPI concentration (from 0.5
379 to 2.0%) and oil content (from 10 to 40%). Many factors can affect the water loss of emulsion
380 gel beads during gelation, such as the concentration of $CaCl_2$ solutions, the water content of
381 original emulsions, the strength of gel matrix, and the hydrophilicity and rigidity of fillers. It
382 has been reported that increasing the concentration of $CaCl_2$ solution (from 0.08 M to 0.3 M)
383 reduced the final weight of alginate gel beads due to the increased water loss (Puguan, et al.,
384 2014), but in this study all samples were dropped into the $CaCl_2$ solutions with the same
385 concentration. Therefore, increasing alginate concentration from 0.5% to 1.5% decreased the
386 water loss of beads from 42.3 ± 1.2% to 36.9 ± 0.3% after gelation (Fig. 3A), which was
387 probably because elastic modulus of gel beads increased with increasing alginate
388 concentration (Fig. 2B), and gels with stronger matric structures had better water-bolding
389 capacity.

In addition, increasing SPI concentration from 0.5% to 2.0% decreased the water loss of emulsion gel beads from 40.2 ± 0.6% to 37.3 ± 0.3% after gelation as well (Figs. 3B), probably due to increased water-absorption capacity of SPI-coated droplets. Denatured SPI has emulsifying capacity because it has both hydrophobic and hydrophilic groups (Nishinari, et al., 2014). As shown in Figs. 1A and 1B, SPI aggregated in sample 1A1S but formed a film at the oil-water interface in sample 1A1S20O, in which hydrophobic groups of SPI connected to oil droplets and hydrophilic groups connected to water. Therefore, more SPI was absorbed at the surface of emulsion droplets by increasing SPI concentration (Fig. 1D), which resulted in increased hydrophilicity of SPI-coated droplets and increased water-retention capacity of emulsion gel beads (Wang, Marcone, Barbut, & Lim, 2012). This explanation could be supported by previous conclusions by Wagner, et al. (1990) that SPI with highly denatured proteins and high surface hydrophobicity exhibited the highest water-absorption capacity. Additionally, increasing oil content from 10% to 40% led to the decreased water loss of emulsion gel beads (from 46.1 ± 0.2% to 25.1 ± 0.4% after gelation) (Figs. 3C), probably because the water content in original emulsions significantly decreased with increasing oil contents from 10% to 40%, and emulsion droplets could protect gel structures from collapse as well. A similar finding has been reported where increasing the oil volume fraction (13%–31.1%) in *β*-lactoglobulin-based oil-in-water emulsions improved the water-retention capacity of emulsion gels (Line, Remondetto, & Subirade, 2005).

3.4 Morphological properties and shrinkage of gel beads

As shown in Fig. 4, alginate gel beads (1A) were transparent, but the presence of SPI decreased the transparency of alginate gel beads (1A1S) because of its yellow colour, and introducing oil led to ivory gel beads, due to the formation of emulsions. In addition, gel beads in all groups were not completely spherical, and samples 1.5A1s20O, 1A2S20O, and 1A1S40O had small tails. This was because increasing the concentrations of alginate, SPI and

oil could raise the viscosity of emulsions (Fig. 5), which could affect the morphological properties of emulsion gel beads. In this study, we used the simple dripping method to produce emulsion gel beads. The emulsions were pushed out from pipette and one droplet was formed at the tip before the droplet grew in size gradually and dropped into $CaCl_2$ solutions. During this process, spherical emulsion droplets were formed because of the surface tension of liquid (Ching, et al., 2017). However, Lević, et al. (2015) found that D-limonene could increase the viscosity and reduce the conductivity of the alginate liquid systems by changing structural ordering of alginate, which indicates that the high viscosity of emulsion was against the formation of spherical bead at the tip of pipet because of poor flow properties. For example, the introduction of hydroxypropylmethylcellulose (0.2%–1%) changed the rheological properties of 2% alginate solutions and produced beads with small tails (Bellich, Borgogna, Cok, and Cesàro, 2011).

Fig. 4 also shows that the size of all samples decreased during gelation and, in order to compare their shrinkage during gelation, the section shrinkage rates were calculated (Fig. 6). The profiles of shrinkage rates show that shrinkage rates of all samples increased during gelation, probably due to syneresis (i.e., water loss) and structural collapse (Rehm, 2009). However, in terms of the profiles of shrinkage rate, increasing contents of alginate and oil could slow the shrinkage, but increasing SPI content had no significant effect on the rate of shrinkage during gelation. Fig.6 also shows that the shrinkage rates decreased from 26.7 ± 2.1% to 18.2 ± 2.2% and from 27.1 ± 1.6% to 13.6 ± 2.5% after gelation with increasing concentrations of alginate (from 0.5% to 1.5%) and oil (from 10% to 40%), respectively, but increasing SPI concentration from 0.5% to 2.0% had no significant effect on the shrinkage rates of emulsion gel beads after gelation for 30 min. Many factors can affect the shrinkage of emulsion gels during gelation, such as water loss, gel stiffness, the content and properties of fillers, and interactions between fillers and the continuous phase (Smith, Scherer, &

Anderson, 1995). In terms of alginate, increasing its concentration could increase the elastic modulus of emulsion gel beads (Fig. 2B), which may provide resistance to shrinkage (Brinker, et al., 1994). Increasing oil concentration led to more compact filler structures, which resisted further shrinkage during gelation as seen on comparing emulsion gel structures of samples 1A1S20O and 1A1S40O in Fig. 1. Eichler, Ramon, Ladyzhinski, Cohen, & Mizrahi (1997) also indicated similar conclusions, in that fructose or polydextrose being introduced into polyacrylamide (PAAm) gels could act as a mechanical barrier against further volume shrinkage of PAAm gels during dehydration. However, increasing SPI concentration reduced the Young's modulus (Fig. 2C) but increased water retention (i.e., decreased water loss) (Fig. 3B) of emulsion gel beads, which may explain why increasing SPI concentration had no significant effects on shrinkage rates of emulsion gel beads.

4. Conclusions

The Young's modulus of alginate-based emulsion gel beads kept increasing before reaching a plateau during gelation process. This gelation process was accompanied by syneresis (i.e., water loss) and shrinkage, which resulted in an increased compactness of emulsion gel beads. SPI-coated droplets could maintain their structures during gelation. With increasing alginate concentration (0.5%–1.5%), the water loss decreased, the Young's modulus increased, and shrinkage rate decreased. Increasing SPI concentration (0.5%–2.0%) led to decreased Young's modulus and water loss, and undifferentiated shrinkage. Higher oil content (10%–40%) decreased water loss and section shrinkage rates, and had no significant effect on the Young's modulus. These findings underlined the effect of concentrations of components on the properties of emulsion gel beads during gelation, which are very important because the properties of emulsion gel beads may affect encapsulation, stability, and release of hydrophobic functional ingredients encapsulated in emulsion gel beads.

Acknowledgement

This work is supported by the China Scholarship Council (No. 201708350111) and Teagasc-The Irish Agriculture and Food Development Authority (RMIS6821). The assistance of Helen Slattery with the freeze-drying system and Deirdre Kennedy with confocal scanning laser microscopy is highly appreciated.

References

Bellich, B., Borgogna, M., Cok, M., & Cesàro, A. (2011). Release properties of hydrogels: Water evaporation from alginate gel beads. *Food Biophysics, 6*, 259-266.

Brinker, C. J., Sehgal, R., Hietala, S., Deshpande, R., Smith, D., Loy, D., & Ashley, C. (1994). Sol-gel strategies for controlled porosity inorganic materials. *Journal of Membrane Science, 94*, 85-102.

Brito-Oliveira, T. C., Bispo, M., Moraes, I. C. F., Campanella, O. H., & Pinho, S. C. (2017). Stability of curcumin encapsulated in solid lipid microparticles incorporated in cold-set emulsion filled gels of soy protein isolate and xanthan gum. *Food Research International, 102*, 759-767.

Ching, S. H., Bansal, N., & Bhandari, B. (2016). Rheology of emulsion-filled alginate microgel suspensions. *Food Research International, 80*, 50-60.

Ching, S. H., Bansal, N., & Bhandari, B. (2017). Alginate gel particles–A review of production techniques and physical properties. *Critical Reviews in Food Science & Nutrition, 57*, 1133-1152.

Corstens, M. N., Berton-Carabin, C. C., Elichiry-Ortiz, P. T., Hol, K., Troost, F. J., Masclee, A. A. M., & Schroën, K. (2017). Emulsion-alginate beads designed to control in vitro intestinal lipolysis: Towards appetite control. *Journal of Functional Foods, 34*, 319-328.

Dickinson, E. (2012). Emulsion gels: The structuring of soft solids with protein-stabilized oil droplets. *Food Hydrocolloids, 28*, 224-241.

Eichler, S., Ramon, O., Ladyzhinski, I., Cohen, Y., & Mizrahi, S. (1997). Collapse processes in shrinkage of hydrophilic gels during dehydration. *Food Research International, 30*, 719-726.

Geremias-Andrade, I. M., Souki, N. P. D. B. G., Moraes, I. C. F., & Pinho, S. C. (2017). Rheological and mechanical characterization of curcumin-loaded emulsion-filled gels produced with whey protein isolate and xanthan gum. *LWT - Food Science and Technology, 86*, 166-173.

Guo, Q., Bellissimo, N., & Rousseau, D. (2017). Role of gel structure in controlling in vitro intestinal lipid digestion in whey protein emulsion gels. *Food Hydrocolloids, 69*, 264-272.

Kerner, E. (1956). The elastic and thermo-elastic properties of composite media. *Proceedings of the Physical Society. Section B, 69*, 808.

Kim, K., Gohtani, S., Matsuno, R., & Yamano, Y. (1999). Effects of oil droplet and agar concentration on gel strength and microstructure of o-w emulsion gel. *Journal of Texture Studies, 30*, 319-335.

King, A. (1983). Brown seaweed extracts (alginates). *Food Hydrocolloids, 2*, 115-188.

Lam, R. S., & Nickerson, M. T. (2013). Food proteins: A review on their emulsifying properties using a structure-function approach. *Food Chemistry, 141*, 975-984.

Lević, S., Pajić Lijaković, I., Đorđević, V., Rac, V., Rakić, V., Šolević Knudsen, T., Pavlović, V., Bugarski, B., & Nedović, V. (2015). Characterization of sodium alginate/$_{D}$-limonene emulsions and respective calcium alginate/$_{D}$-limonene beads produced by electrostatic extrusion. *Food Hydrocolloids, 45*, 111-123.

Liang, F., Liu, J., Zhang, C., Qu, X., Li, J., & Yang, Z. (2011). Janus hollow spheres by emulsion interfacial self-assembled sol-gel process. *Chemical Communications, 47*, 1231-1233.

Lin, D., Lu, W., Kelly, A. L., Zhang, L., Zheng, B., & Miao, S. (2017). Interactions of vegetable proteins with other polymers: Structure-function relationships and applications in the food industry. *Trends in Food Science & Technology, 68*, 130-144.

Line, V. L.S., Remondetto, G. E., & Subirade, M. (2005). Cold gelation of *β*-lactoglobulin oil-in-water emulsions. *Food Hydrocolloids, 19*, 269-278.

Ma, D., Tu, Z.-C., Wang, H., Zhang, Z., & McClements, D. J. (2017). Fabrication and characterization of nanoemulsion-coated microgels: Electrostatic deposition of lipid droplets on alginate beads. *Food Hydrocolloids, 71*, 149-157.

Ma, L., Wan, Z., & Yang, X. (2017). Multiple water-in-oil-in-water emulsion gels based on self-assembled saponin fibrillar network for photosensitive cargo protection. *Journal of Agricultural and Food Chemistry, 65*, 9735-9743.

Moschakis, T., Murray, B. S., & Biliaderis, C. G. (2010). Modifications in stability and structure of whey protein-coated o/w emulsions by interacting chitosan and gum arabic mixed dispersions. *Food hydrocolloids, 24*, 8-17.

Natrajan, D., Srinivasan, S., Sundar, K., & Ravindran, A. (2015). Formulation of essential oil-loaded chitosan-alginate nanocapsules. *Journal of Food and Drug Analysis, 23*, 560-568.

Nishinari, K., Fang, Y., Guo, S., & Phillips, G. O. (2014). Soy proteins: A review on composition, aggregation and emulsification. *Food Hydrocolloids, 39*, 301-318.

Oliver, L., Berndsen, L., van Aken, G. A., & Scholten, E. (2015). Influence of droplet clustering on the rheological properties of emulsion-filled gels. *Food Hydrocolloids, 50*, 74–83.

Pintado, T., Ruiz-Capillas, C., Jimenez-Colmenero, F., Carmona, P., & Herrero, A. M. (2015). Oil-in-water emulsion gels stabilized with chia (*Salvia hispanica L.*) and cold gelling agents: Technological and infrared spectroscopic characterization. *Food Chemistry*, 185, 470–478.

Piornos, J. A., Burgos-Díaz, C., Morales, E., Rubilar, M., & Acevedo, F. (2017). Highly efficient encapsulation of linseed oil into alginate/lupin protein beads: Optimization of the emulsion formulation. *Food Hydrocolloids, 63*, 139-148.

Puguan, J. M., Yu, X., & Kim, H. (2014). Characterization of structure, physico-chemical properties and diffusion behavior of Ca-Alginate gel beads prepared by different gelation methods. *Journal of Colloid and Interface Science, 432*, 109-116.

Quong, D., Neufeld, R., Skjåk-Bræk, G., & Poncelet, D. (1998). External versus internal source of calcium during the gelation of alginate beads for DNA encapsulation. *Biotechnology and Bioengineering, 57*, 438-446.

Rehm, B. H. A. (Ed.). (2009). *Alginates: biology and applications*. Heidelberg: Springer.

Rosa, P., Sala, G., Van Vliet, T., & Van De Velde, F. (2006). Cold gelation of whey protein emulsions. *Journal of Texture Studies, 37*, 516-537.

Sala, G., de Wijk, R. A., van de Velde, F., & van Aken, G. A. (2008). Matrix properties affect the sensory perception of emulsion-filled gels. *Food Hydrocolloids, 22*, 353-363.

Sala, G., van Vliet, T., Cohen Stuart, M. A., Aken, G. A. v., & van de Velde, F. (2009). Deformation and fracture of emulsion-filled gels: Effect of oil content and deformation speed. *Food Hydrocolloids*, 23, 1381–1393.

Sato, A. C. K., Moraes, K. E. F. P., & Cunha, R. L. (2014). Development of gelled emulsions with improved oxidative and pH stability. *Food Hydrocolloids*, 34, 184–192.

Smith, D., Scherer, G., & Anderson, J. (1995). Shrinkage during drying of silica gel. *Journal of Non-Crystalline Solids, 188*, 191-206.

Tavernier, I., Patel, A. R., Van der Meeren, P., & Dewettinck, K. (2017). Emulsion-templated liquid oil structuring with soy protein and soy protein: *κ*-carrageenan complexes. *Food Hydrocolloids, 65*, 107-120.

Urbonaite, V., de Jongh, H. H. J., van der Linden, E., & Pouvreau, L. (2015). Water holding of soy protein gels is set by coarseness, modulated by calcium binding, rather than gel stiffness. *Food Hydrocolloids, 46*, 103-111.

Van Vliet, T. (1988). Rheological properties of filled gels: Influence of filler matrix interaction. *Colloid and Polymer Science, 266*, 518-524.

Vasile, F. E., Judis, M. A., & Mazzobre, M. F. (2018). Impact of Prosopis alba exudate gum on sorption properties and physical stability of fish oil alginate beads prepared by ionic gelation. *Food Chemistry, 250*, 75-82.

Wagner, J., & Añón, M. C. (1990). Influence of denaturation, hydrophobicity and sulfhydryl content on solubility and water absorbing capacity of soy protein isolates. *Journal of Food Science, 55*, 765-770.

Wang, S., Marcone, M., Barbut, S., & Lim, L. T. (2012). The impact of anthocyanin-rich red raspberry extract (ARRE) on the properties of edible soy protein isolate (SPI) films. *Journal of Food Science, 77*, C497-505.

570 Wang, Z., Neves, M. A., Kobayashi, I., Uemura, K., & Nakajima, M. (2013). Preparation,
571 characterization, and in vitro gastrointestinal digestibility of oil-in-water emulsion-agar gels.
572 *Bioscience Biotechnology and Biochemistry, 77*, 467-474.
573 Yang, N., Feng, Y. N., Su, C. X., Wang, Q., Zhang, Y. M., Wei, Y. H., Zhao, M., Nishinari, K., Fang,
574 Y. P. (2020). Structure and tribology of *κ*-carrageenan gels filled with natural oil bodies. *Food*
575 *hydrocolloids*, 105945.
576 Yin, L., Zhao, Z., Hu, Y., Ding, J., Cui, F., Tang, C., & Yin, C. (2008). Polymer–protein interaction,
577 water retention, and biocompatibility of a stimuli-sensitive superporous hydrogel containing
578 interpenetrating polymer networks. *Journal of Applied Polymer Science*, *108*, 1238-1248.
579 Zhang, Z. P., Zhang, R. J., Zou, L. Q., Chen, L., Ahmed, Y., Bishri, W. A., Balamash, K., &
580 McClements, D. J. (2016). Encapsulation of curcumin in polysaccharide-based hydrogel
581 beads. *Food Hydrocolloids*, *58*, 160–170.
582

583 **Table 1**

584 Formulations of experimental emulsions.

Group	Water phase[a]		Oil Con. (% wt)
	Alginate Con. (% wt)	Soy protein Con. (% wt)	
1A (Control 1)	1.0	0	0
1A1S (Control 2)	1.0	1.0	0
1A1S20O	1.0	1.0	20
0.5A1S20O	0.5	1.0	20
1.5A1S20O	1.5	1.0	20
1A0.5S20O	1.0	0.5	20
1A2S20O	1.0	2.0	20
1A1S10O	1.0	1.0	10
1A1S40O	1.0	1.0	40

585 [a] The content of water phase was adjusted according to the oil content in the formulation.

Figure Legends

Fig. 1. CLSM images of dispersions/emulsions (A–E) and gel beads (V–Z) after gelation for 30 min. SPI and sunflower oil were stained by red and green, respectively.

Fig. 2. Kinetics of Young's modulus of alginate-based gel beads during gelation: (A) control groups; (B) effect of alginate concentrations (0.5–1.5% in the water phase); (C) effect of SPI concentrations (0.5–2.0% in the water phase); and (D) effect of oil contents (10–40% in the emulsion).

Fig. 3. Kinetics of water loss from alginate-based gel beads during gelation: (A) effect of alginate concentrations (0.5–1.5% in the water phase); (B) effect of SPI concentrations (0.5–2.0% in the water phase); and (C) effect of oil contents (10–40% in the emulsion).

Fig. 4. Visual aspects of alginate-based gel beads during gelation (minimum scale mark = 1 mm).

Fig. 5. Viscosity of dispersions/emulsions with different component concentrations.

Fig. 6. Kinetics of section shrinkage of alginate-based gel beads during gelation: (A) effect of alginate concentrations (0.5–1.5% in the water phase); (B) effect of SPI concentrations (0.5–2.0% in the water phase); and (C) effect of oil contents (10–40% in the emulsion).

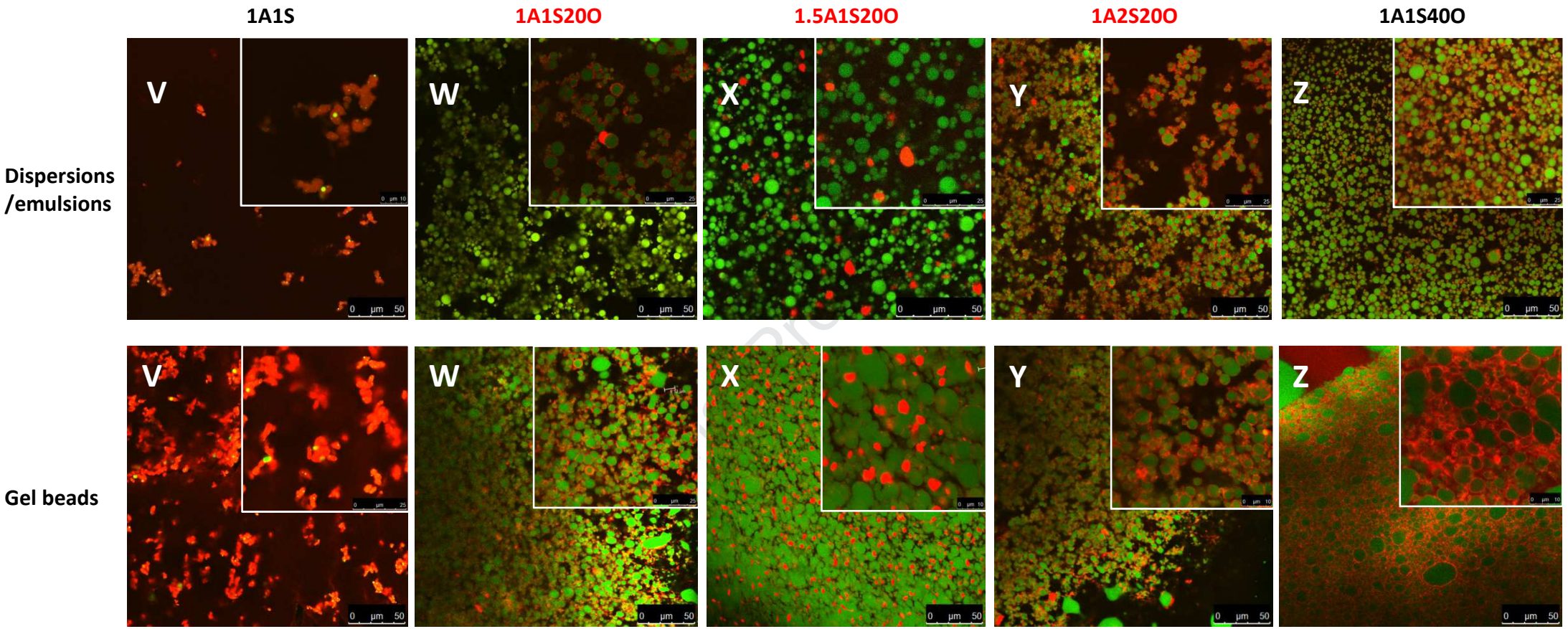
1A1S
1A1S20O
1.5A1S20O
1A2S20O
1A1S40O
Dispersions /emulsions
Gel beads
V
W
X
Y
Z

Fig. 1

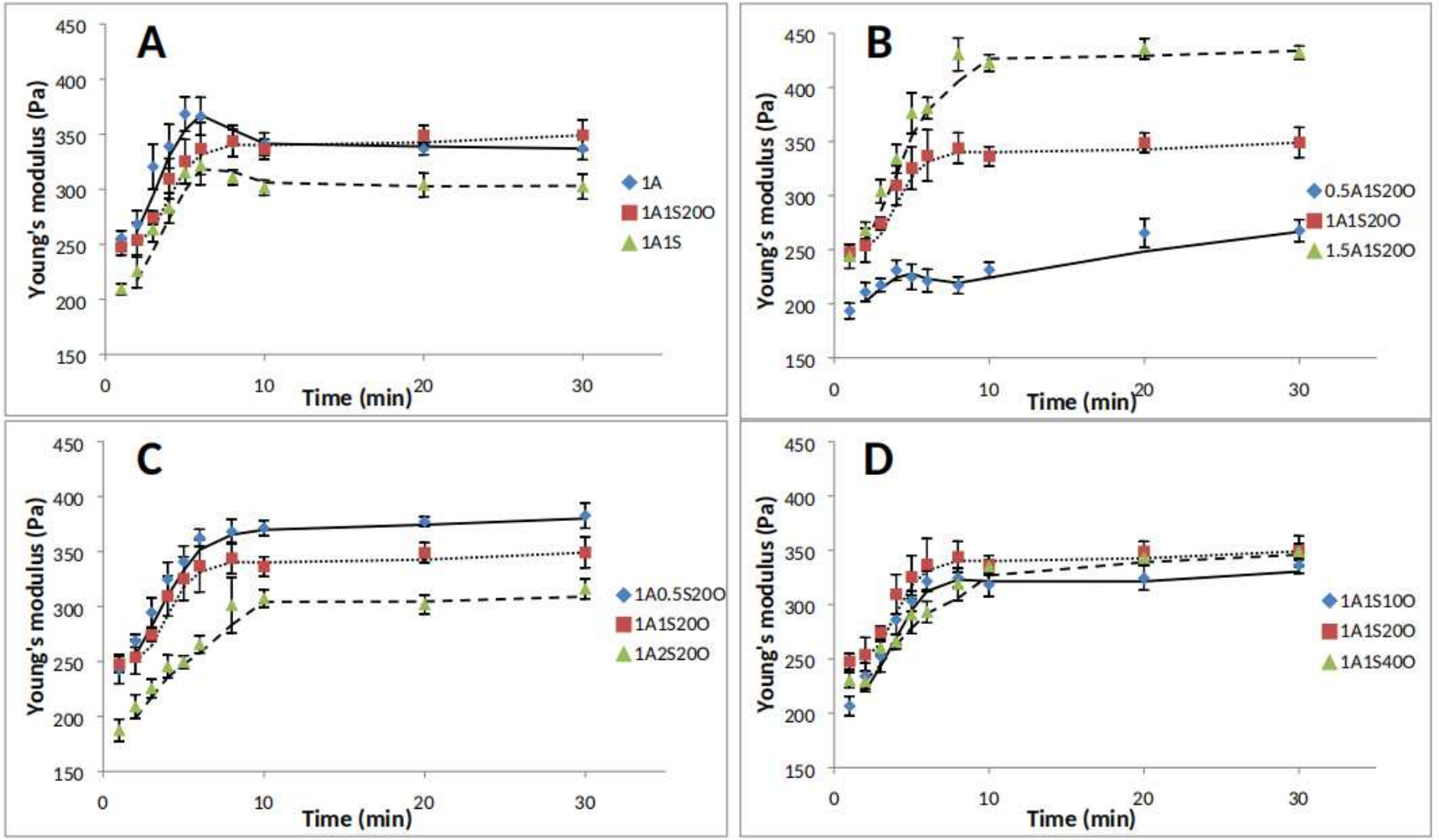
A
Young's modulus (Pa)
Time (min)
1A
1A1S20O
1A1S
B
Young's modulus (Pa)
Time (min)
0.5A1S20O
1A1S20O
1.5A1S20O
C
Young's modulus (Pa)
Time (min)
1A0.5S20O
1A1S20O
1A2S20O
D
Young's modulus (Pa)
Time (min)
1A1S10O
1A1S20O
1A1S40O

Fig. 2

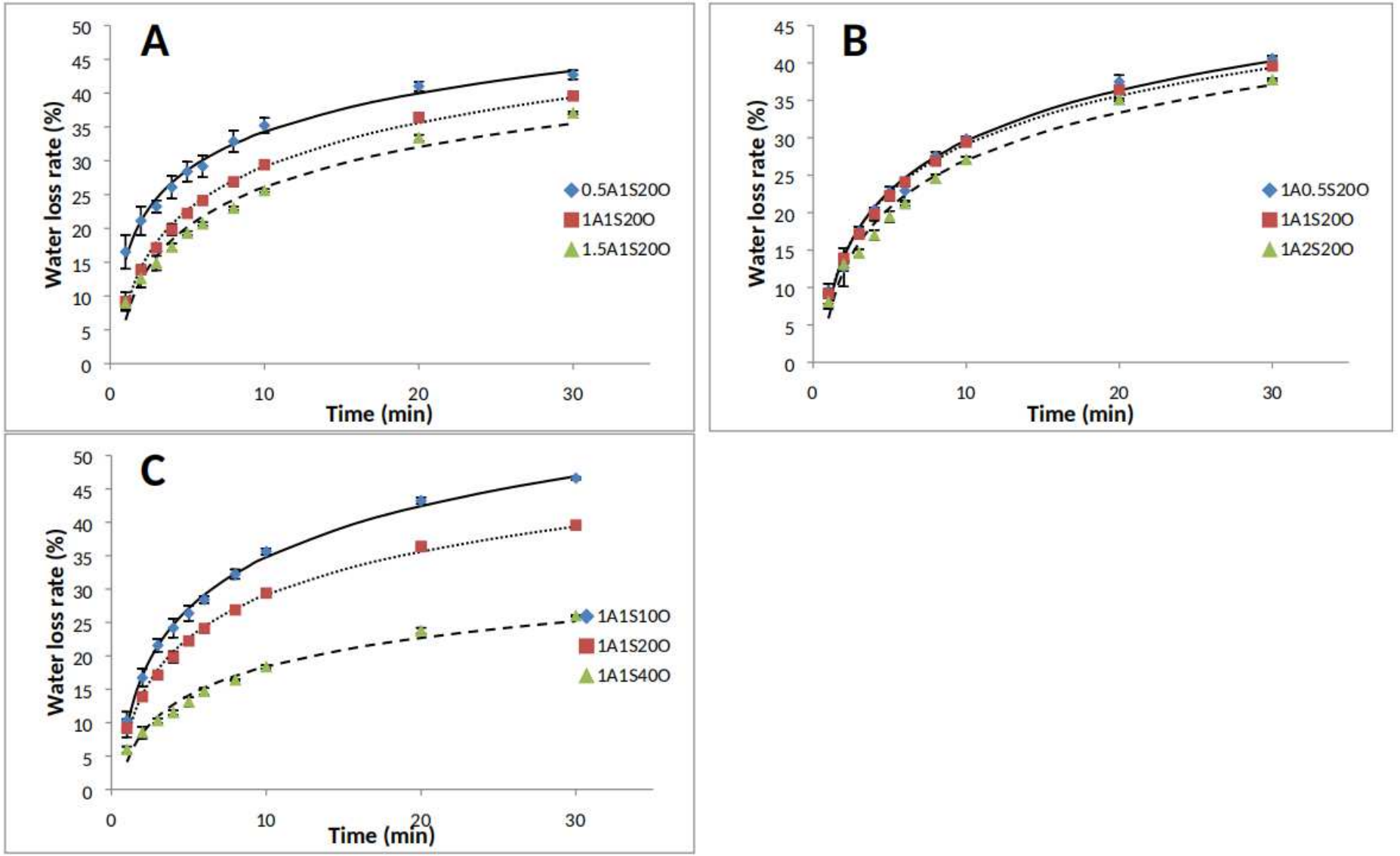
A
Water loss rate (%)
Time (min)
0.5A1S20O
1A1S20O
1.5A1S20O
B
Water loss rate (%)
Time (min)
1A0.5S20O
1A1S20O
1A2S20O
C
Water loss rate (%)
Time (min)
1A1S10O
1A1S20O
1A1S40O

Fig. 3

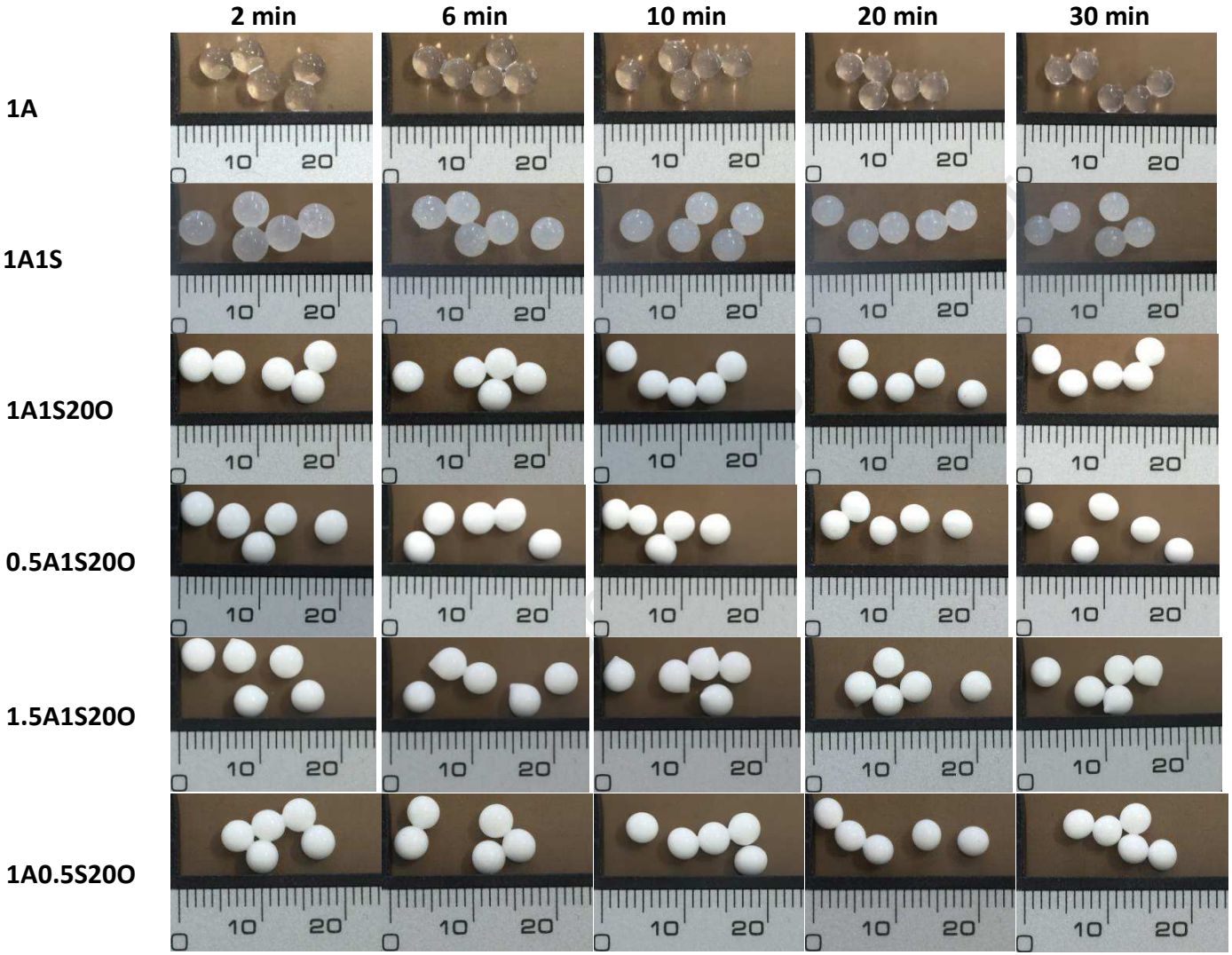
2 min
6 min
10 min
20 min
30 min
1A
1A1S
1A1S20O
0.5A1S20O
1.5A1S20O
1A0.5S20O

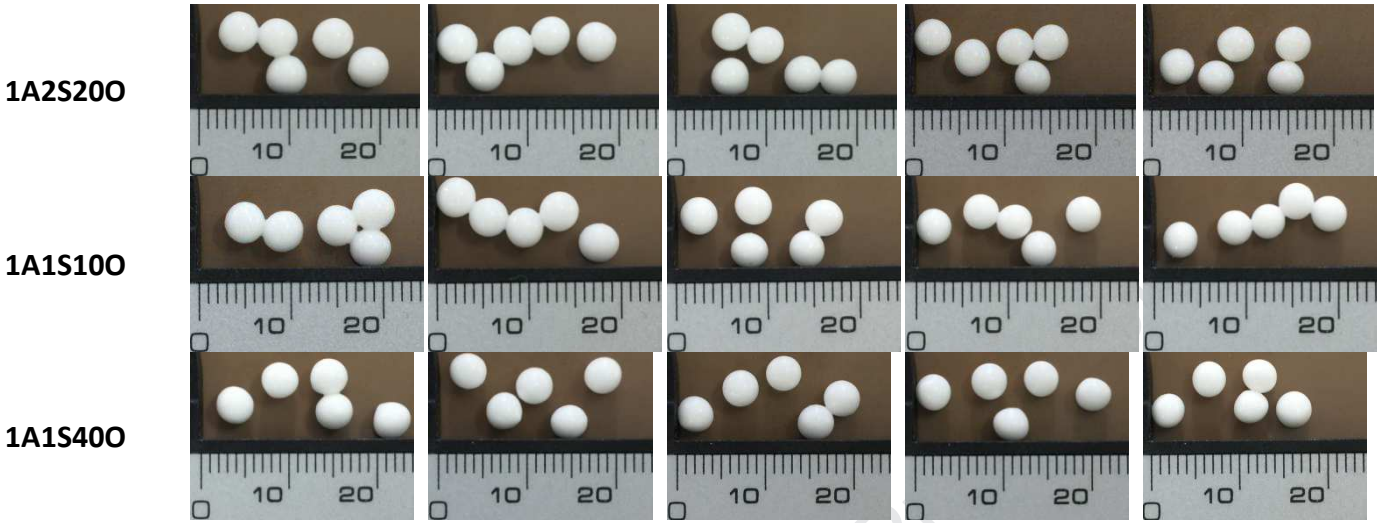

Fig. 4

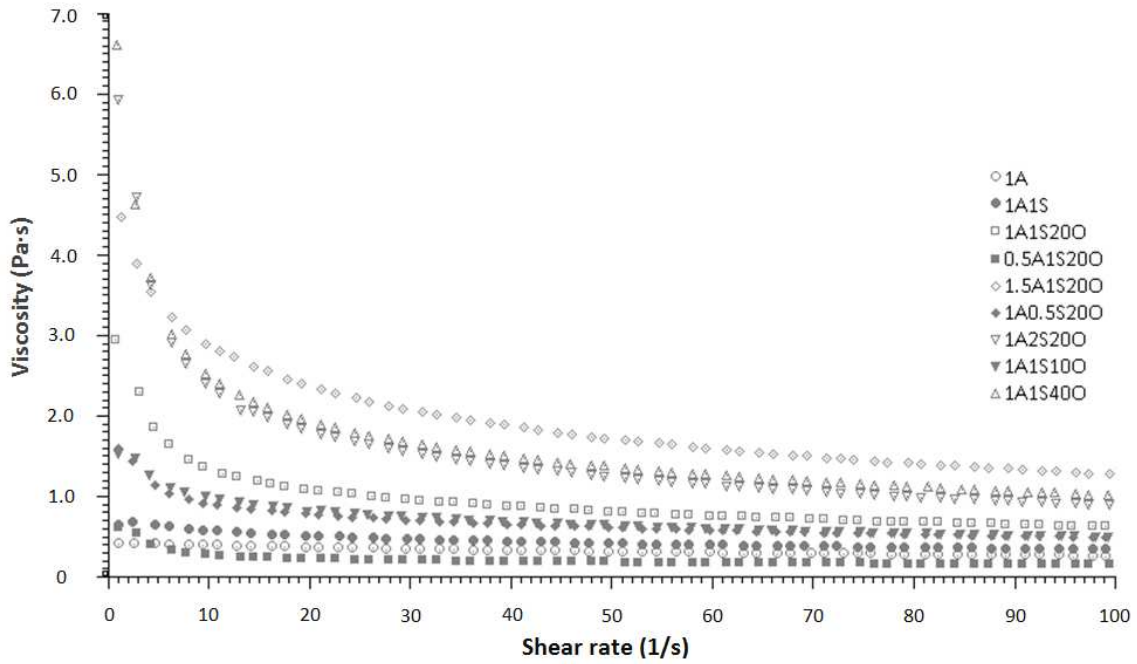
Viscosity (Pa·s)
Shear rate (1/s)
1A
1A1S
1A1S20O
0.5A1S20O
1.5A1S20O
1A0.5S20O
1A2S20O
1A1S10O
1A1S40O

Fig. 5

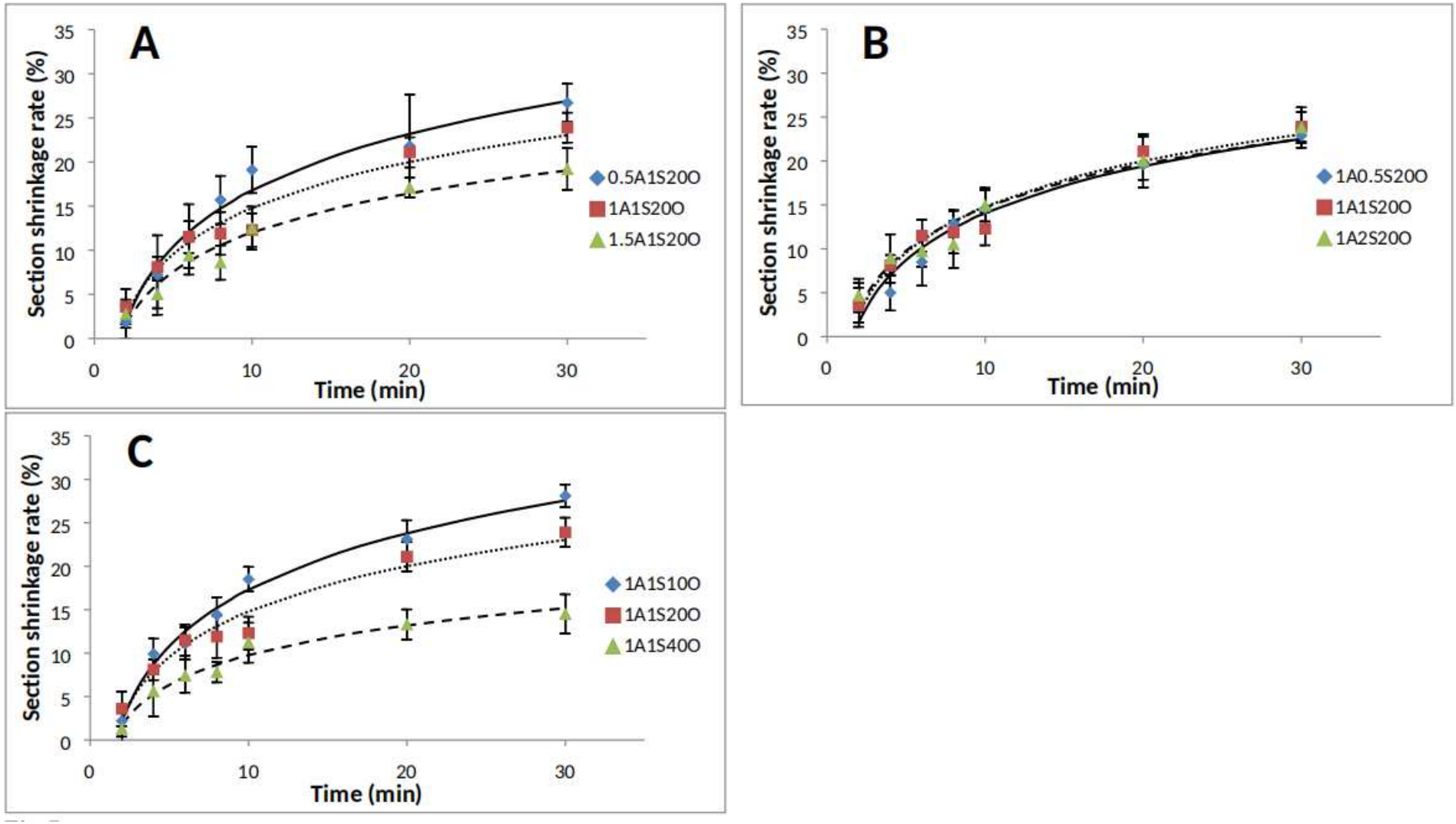
A
Section shrinkage rate (%)
Time (min)
0.5A1S20O
1A1S20O
1.5A1S20O
B
Section shrinkage rate (%)
Time (min)
1A0.5S20O
1A1S20O
1A2S20O
C
Section shrinkage rate (%)
Time (min)
1A1S10O
1A1S20O
1A1S40O

Fig. 6

Highlights

• The Young's modulus of emulsion gel beads increased before reaching a plateau during gelation.

• The gelation of emulsion gel beads was accompanied by syneresis and shrinkage.

• High SPI and oil content led to re-coalescence of emulsion droplets during gelation.

• Increasing SPI content decreased the Young's modulus of emulsion gel beads.

• Increasing oil content decreased the shrinkage of emulsion gel beads.

Duanquan Lin: Conceptualization, Methodology, Writing - original draft, Data curation, investigation.

Alan Kelly: Supervision, writing - review & editing.

Valentyn Maidannyk: Investigation.

Song Miao: Supervision, Conceptualization, Writing - review & editing, Funding acquisition, Project administration, Investigation.

Declaration of interests

☒ The authors declare that they have no known competing financial interests or personal relationships that could have appeared to influence the work reported in this paper.

☐The authors declare the following financial interests/personal relationships which may be considered as potential competing interests:

Song Miao

Teagasc Food Research Centre, Moorepark